SPANDIDOS PUBLICATIONS

ONCOLOGY LETTERS 17: 5175-5186, 2019

Effect of the Nrf2-ARE signaling pathway on biological characteristics and sensitivity to sunitinib in renal cell carcinoma

SHILIANG JI[1], YUFENG XIONG[2], XINGXING ZHAO[3], YANLI LIU[4] and LI QIANG YU[5]

[1]Department of Pharmacy, Suzhou Science and Technology Town Hospital, The Affiliated Suzhou Hospital of Nanjing Medical University, Suzhou, Jiangsu 215153; [2]Department of Clinical Laboratory, Guangdong Women and Children Health Hospital, Guangzhou, Guangdong 510000; [3]Department of Neonatology, Suzhou Municipal Hospital, The Affiliated Suzhou Hospital of Nanjing Medical University, Suzhou, Jiangsu 215000; [4]College of Pharmaceutical Science, Soochow University, Suzhou, Jiangsu 215123; [5]Department of Neurology, The First Affiliated Hospital of Soochow University, Suzhou, Jiangsu 215000, P.R. China

Received May 7, 2018; Accepted January 17, 2019

DOI: 10.3892/ol.2019.10156

Abstract. The aim of the present study was to examine the effects of the nuclear factor erythroid-2 related factor 2-antioxidant-responsive element (Nrf2-ARE) signaling pathway on the biological characteristics and sensitivity to targeted therapy in human renal cell carcinoma (RCC) cells. RCC tissues and adjacent tissues were collected and assessed by immunohistochemistry to determine the expression of Nrf2, NAD(P)H dehydrogenase [quinone] 1 (NQO1) and heme oxygenase-1 (HO-1) to analyze the clinicopathological features of RCC. A series of *in vitro* experiments were conducted to analyze the biological characteristics of Nrf2-ARE signaling in RCC. The renal cancer cell line, 786-0 was used, and cells was divided into a mock group, negative control group and small hairpin (sh)RNA-Nrf2 group. A Cell Counting Kit-8 assay was performed alongside flow cytometry to detect cell viability, cell cycle stage and apoptosis following treatment with sunitinib. The results demonstrated that Nrf2, NQO1 and HO-1 were significantly upregulated in RCC tissues compared with adjacent tissues and were associated with tumor node metastasis stage, Fuhrman classification and lymph node metastasis. Following shRNA-Nrf2 transfection, the 786-0 cells demonstrated a significant decrease in viability, cell invasion and scratch healing rate, and the mRNA and protein expression levels of Nrf2, NQO1, HO-1 and glutathione transferase were significantly decreased, which enhanced the sensitivity to sunitinib, arrested cells in the G0/G1 phase and increased apoptosis. In conclusion, Nrf2-ARE signaling is important for RCC progression, and its inhibition may increase sensitivity to targeted drugs to provide novel developments for RCC treatment.

Correspondence to: Dr Li Qiang Yu, Department of Neurology, The First Affiliated Hospital of Soochow University, 899 Ping Hai Road, Suzhou, Jiangsu 215000, P.R. China
E-mail: yuliqiang@suda.edu.cn

Key words: nuclear factor erythroid-2 related factor 2-antioxidant-responsive element signaling pathway, 786-0 cells, sunitinib, oncotherapy

Introduction

With annually increasing morbidity and mortality rates, renal cell carcinoma (RCC) accounts for ~90% of all renal malignancies and represents 2-3% of all human cancer types (1,2). In the early stages of RCC, patients do not exhibit specific clinical symptoms, including mass, hematuria and local pain, and 20-30% of all patients are diagnosed with the metastatic disease (3). Generally, radical surgery may achieve positive therapeutic results; however, metastasis is observed in 20-40% of patients with localized or locally advanced RCC who undergo early radical surgery (4). Advanced metastatic RCC responds poorly to simple excision, is insensitive to chemotherapy and is prone to develop drug resistance, with only 7-10% efficiency for chemotherapeutic drugs (5). Therefore, the recommended conventional therapies are primarily immunotherapy and targeted drug therapy (6). With the progression of molecular genetics in the study of RCC, there has been rapid development in molecular targeted therapy, targeting cell receptors, tumor-associated genes and signaling pathways. Accumulating clinical evidence demonstrated that targeted drugs may improve the prognosis of patients with RCC (7,8).

Previously, novel micromolecular-targeted drugs, including sunitinib, markedly improved the therapeutic prospect of patients with advanced RCC, contributing to a marked increase in the survival rate and total remission rate of patients with RCC (9,10). However, a considerable proportion of patients with RCC are not able to experience clinical benefits, and the majority of patients develop drug resistance or even RCC progression, typically in the first 6-15 months after therapy, due to the severe limitations of targeted drug resistance on therapeutic effects (11,12).

Nuclear factor erythroid-2 related factor 2 (Nrf2), a key transcription factor, activates the endogenous antioxidant response by regulating cellular antioxidant stress (13). The antioxidant-responsive element (ARE) is a promoter sequence

located in the upstream regulatory region of certain protective genes, which may be activated by Nrf2 (14). When Nrf2 is activated by toxic and harmful substances, it translocates to the nucleus and interacts with ARE to activate Nrf2-ARE target genes, leading to the regulation of downstream antioxidant proteins, oxidases and phase II detoxifying enzymes (15). Nrf2-ARE signaling promotes tumor growth and induces drug resistance in non-small-cell lung cancer, and inhibition of Nrf2 signaling significantly suppressed colon tumor cell growth (16,17). Samatiwat *et al* (18) identified that suppression of Nrf2-regulated genes via small interfering (si)RNA increased the sensitivity to 5-fluorouracil and gemcitabine in cholangiocarcinoma cells. Additionally, Akhdar *et al* (19) demonstrated that suppression of Nrf2 via a drug inhibitor or siRNA transfection increased the sensitivity to chemotherapy drugs, including 5-fluorouracil, in colorectal cancer.

However, the role of Nrf2-ARE signaling in RCC and its detailed molecular mechanism remain unknown. Therefore, the present study was conducted to examine how Nrf2-ARE signaling affects the biological characteristics of RCC and sensitivity to sunitinib, to provide a novel theoretical basis to better predict the prognosis of patients with RCC and to select targeted drugs.

Materials and methods

Study subjects. The protocol in the present study was approved by the Ethics Committee of The First Affiliated Hospital of Soochow University, Suzhou, China (approval no. 2013031), and all research subjects provided written informed consent. All procedures in the present study strictly complied with the guidelines and principles of the Declaration of Helsinki. Between January 2010 and January 2012, a total of 108 patients with RCC from The First Affiliated Hospital of Soochow University (Suzhou China), who received radical nephrectomy were enrolled in the present study, consisting of 78 males and 30 females aged between 31 and 78 years (mean age: 52.90±14.01 years). All subjects were diagnosed with RCC by pathological examination following surgery. Adjacent tissues, 4 cm away from carcinoma tissues were selected for the control group. The inclusion criteria were as follows: Complete pathology reports and other associated data, did not receive radiotherapy, chemotherapy or immunotherapy prior to surgery, did not possess tumors in other parts of the body, and did not have a previous history of diseases of the heart, liver, kidney or other systems. According to pathological type, 81 patients had renal clear cell carcinoma; eight patients had granular cell basal cell carcinoma; 14 patients had papillary RCC; and five patients had other types of RCC. Based on the Fuhrman histological classification of RCC, 66 cases were in grade I + II and 42 cases in grade III + IV (20). On the basis of the Tumor Node Metastasis (TNM) staging system designed by the Union for International Cancer Control in 2009, 35 cases were in stage I; 29 cases were in stage II; 30 cases were in stage III and 14 cases were in stage IV; and 29 cases had lymph node metastasis, whereas, 79 cases did not (21).

Immunohistochemistry. Tissue specimens collected from all the patients with RCC were fixed in 4% paraformaldehyde for 5 min at room temperature, embedded in paraffin and cut into 3 μm sections. The sections were deparaffinized in xylene and dehydrated in 100, 90, 70, and 50% alcohol solutions (5 min each at 37˚C), followed by antigen retrieval in a citrate solution of pH 7.2-7.4. The sections were then blocked in 10% normal donkey serum (Chemicon International; Thermo Fisher Scientific, Inc., Waltham, MA, USA) in PBS at 37˚C for 30 min. Primary antibodies used were rabbit monoclonal antibodies for Nrf2 (cat. no., sc-365949, Santa Cruz Biotechnology, Inc., Dallas, TX, USA), NAD(P)H dehydrogenase [quinone] 1 (NQO1, cat. no., sc-376023; Santa Cruz Biotechnology, Inc.) and heme oxygenase-1 (HO-1; cat. no., sc-136960; Santa Cruz Biotechnology, Inc., Dallas, TX, USA) at 1:100 dilution, which were incubated with tissue sections at 4˚C overnight. Following incubation with the primary antibodies, the sections were washed with PBS (0.01 mol/l). The biotinylated secondary antibody (1 mg/ml; cat. no., BA1080; Wuhan Boster Biological Technology Co., Ltd., Wuhan, China) was added, followed by a 30-min incubation at 37˚C, 10-min diaminobenzidine staining at 37˚C, counterstaining with hematoxylin for 30 sec at 37˚C, dehydration with 100, 90, 70, and 50% alcohol (5 min each at 37˚C), clearing and mounting with neutral gum. The sections were observed under a light microscope (magnification, x200). Parameters were calculated using Image-Pro Plus 6.0 (Media Cybernetics, Inc., Rockville, MD, USA) pathological image analysis software for statistical analysis.

The positive expression of Nrf2, NQO1 and HO-1 was determined by a score and a semi-quantitative method in the cytoplasm (22). Under high magnification, 10 fields (100 cells/field) were randomly selected to calculate the average percentage of positive cells in each field per section as follows: i) 0 for no positive cells; ii) 1 for <10% positive cells; iii) 2 for 10-50% positive cells; iv) 3 for 50-80% positive cells; and v) 4 for 80-100% positive cells. Based on the staining characteristics of the majority of positive cells, the staining intensity was scored as: i) 0 for no intensity; ii) 1 for light yellow; iii) 2 for pale brown; iv) and 3 for sepia. The score of the average positive cell was multiplied by the score of staining intensity: 1-3 for negative and 4-12 for positive.

Follow-up. The five-year overall survival (OS) rate was determined from the date of diagnosis. The follow-up was conducted via outpatient service, telephone calls or medical records. The OS rate was defined as the time from the date of first surgery until mortality or the last follow-up, and the survival time was calculated monthly.

Cell selection and culture. Human RCC cells (ACHN, Caki-1, 769-P and 786-0) were purchased from the Cell Resource Center of Shanghai Institute of Life Science (Shanghai, China) and human kidney tubule epithelia cells (HK-2) were obtained from The American Type Culture Collection, Manassas, VA, USA. All cells were cultured in RPMI-1640 culture solution (Gibco; Thermo Fisher Scientific, Inc.), containing 10% fetal bovine serum (Gibco; Thermo Fisher Scientific, Inc.), 100 U/ml penicillin and 100 μg/ml streptomycin. All cells were cultured at 37˚C in an incubator with 5% CO_2, followed by passages when cell confluence reached 80-90% and passaging once every 2-3 days. Cells in the logarithmic phase were inoculated in 6-well plates at $3x10^3$ cells/well for further experiments.

Cell grouping and transfection. The 786-0 cells were divided into three groups; the mock group (blank group of 786-0 cells), the negative control (NC) group (786-0 cells transfected with empty plasmid) and the small hairpin (sh) RNA-Nrf2 group (786-0 cells transfected with shRNA-Nrf2 plasmid). The cells in the logarithmic phase in each group were inoculated in 6-well plates at $4x10^5$ cells/well and transfected with Lipofectamine® 3000 (cat no. L3000015; Invitrogen; Thermo Fisher Scientific, Inc.) according to the manufacturer's protocol. The shRNA-Nrf2 plasmid and empty plasmid (200 ng, purchased from OriGene Technologies, Inc., Beijing, China) were diluted with Opti-Minimum Essential Medium (MEM; Sigma-Aldrich; Merck KGaA, Darmstadt, Germany). The diluted plasmid and Lipofectamine® 3000 were added to 100 μl Opti-MEM, mixed and added to 6-well plates (200 μl/well). After transfection for 6-8 h, the media was changed and the cells were incubated at 37˚C with 5% CO_2. Further experiments were conducted at 48 h following transfection.

Cell Counting Kit-8 (CCK-8) assay. The 786-0 cells in the logarithmic phase in each group were washed with PBS, digested with trypsin and made into a cell suspension. Subsequently, 100 μl cell suspension was added to each well and incubated for 12, 24, 48 or 72 h at 37˚C in a CO_2 incubator. Each group had three parallel control wells. A total of 10 μl CCK-8 reagent (cat. no. CK04; Dojindo Molecular Technologies, Inc., Shanghai, China) was added for 1 h incubation. The optical density (OD) value at 450 nm was measured using a microplate reader (Thermo Fisher Scientific, Inc.). Each experiment was repeated three times to obtain the average OD value. Additionally, the transfected 786-0 cells had 24, 48 and 72 h cultures in different concentrations of sunitinib (0.1, 0.2, 0.5, 1.0, 2.0, 5.0 and 10 μmol/l). The cell viability was calculated using the following equation: OD value of the experimental group/OD value of the blank group x100. The cell viability was additionally used to calculate the half maximal inhibitory concentration (IC_{50}).

Matrigel™ chamber invasion assay. Following melting at 4˚C, Matrigel™ was diluted to a 1:3 ratio with serum-free Dulbecco's modified Eagle's medium (DMEM; Invitrogen; Thermo Fisher Scientific, Inc.), mixed and added into each upper chamber and dried at room temperature. Following digestion with trypsin, 786-0 cells in each group were added to serum-free DMEM to make cell suspensions at a density of $1x10^5$ cells/ml for 24-h culture. The 786-0 cell suspension was added to the upper chamber (200 μl per chamber), and 500 μl DMEM containing 10% fetal bovine serum (Hyclone; GE Healthcare Life Sciences, Logan, UT, USA) was added to 24-well plates without introducing air bubbles. A Transwell chamber was placed into each well. Following a 20 h routine culture, the chamber was removed and washed with PBS. Following culture removal, the residual Matrigel™ and 786-0 cells in the chamber microporous membrane were wiped with a cotton swab, followed by a 15-min fixation at 37˚C in 95% alcohol and crystal violet staining for 5 min at 37˚C. The average number of 786-0 cells crossing the membrane was observed under an inverted light microscope (magnification, x200).

Scratch assay. Cells in each group were seeded into 6-well plates at $5x10^4$ cells/well. Following adherence to the surface, cells were scratched gently with a 2 mm spatula. The cells were subsequently rinsed with PBS and cultured in serum-free DMEM for 24 h. Scratch wound healing was observed under an inverted light microscope (x200) and imaged at 0 and 24 h. Image-Pro Plus 6.0 software was used to measure the distance between two scratches. The scratch-healing rate was calculated as follows: (distance at 1-24 h/distance at 0 h) x 100.

Reverse transcription-quantitative polymerase chain reaction (RT-qPCR). Total RNA of the 786-0 cells was extracted with a TRIzol reagent kit (Qiagen, Inc., Valencia, CA, USA), according to the manufacturer's protocol. cDNA was synthesized from 200 ng of total RNA by reverse transcription using a Transcriptor First-Strand cDNA Synthesis kit (Roche Diagnostics, Basel, Switzerland). According to the gene sequences of the GenBank database (https://www.ncbi.nlm.nih.gov/pubmed/), the primers were designed using Primer Premier 5.0 software (Premier Biosoft International, Palo Alto, CA, USA; Table I) and were synthesized by Shanghai Sangon Pharmaceutical Co., Ltd., (Shanghai, China). Each 20 μl PCR system consisted of 10 μl SYBR PremixExTaq (Takara Bio, Inc., Otsu, Japan), 0.8 μl 10 nM forward primer, 0.8 μl 10 nM reverse primer, 0.4 μl ROX reference dye II, 2 μl DNA template and 6.0 μl dH_2O. The RT-qPCR was conducted under the following conditions: 40 cycles of 30 sec predenaturation at 95˚C, 5 sec denaturation at 95˚C, 30 sec annealing at 60˚C and 30 sec extension at 72˚C. GAPDH was used as an internal reference. The quantification cycle (Cq) for the relative expression of target gene was calculated using the relative quantitative $2^{-\Delta\Delta Cq}$ method (23,24).

Western blotting. Total protein of the 786-0 cells was extracted using the Bicinchoninic Acid Protein Assay kit (cat. no. AR0146; Wuhan Boster Biological Technology Co., Ltd.) to detect the protein concentration. The loading buffer was added to the extracted proteins, following boiling at 95˚C for 10 min. A total of 30 μg proteins was loaded in each well of a 10% polyacrylamide gel. Gel electrophoresis was run at 80 and 120 V, followed by a wet transfer at 100 mV for 45-70 min to polyvinylidene difluoride (PVDF) membranes. Following a 1 h incubation with 5% bovine serum albumin (Hyclone; GE Healthcare Life Sciences) at room temperature, PVDF membranes were incubated with primary antibodies against Nrf2 (cat. no. sc-365949; Santa Cruz Biotechnology, Inc.), NQO1 (cat. no. sc-376023; Santa Cruz Biotechnology, Inc.), HO-1 (cat. no. sc-136960; Santa Cruz Biotechnology, Inc.) or glutathione S-transferase (GST; cat. no. sc-53909; Santa Cruz Biotechnology, Inc.) at a 1:1,000 dilution and GAPDH (cat. no. 5174; Cell Signaling Technology, Inc., Danvers, MA, USA) at 1:5,000 dilution at 4˚C overnight, and washed with TBS with Tween-20 (TBST) three times (5 min/time). The membranes were subsequently incubated with the HRP-conjugated anti-mouse IgG secondary antibody (cat. no. sc-51625; 1:3,000 dilution; Santa Cruz Biotechnology, Inc.) at room temperature for 1 h. The membranes were washed with TBST three times (5 min/time) and chemiluminescence reagent (ECL Plus; GE Healthcare) was added to develop using a Bio-Rad Gel Dol EZ imager (GEL DOC EZ IMAGER; Bio-Rad Laboratories, Inc.,

Table I. Primer sequences for quantitative PCR.

PCR primer sequences	Forward, 5'-3'	Reverse, 5'-3'
Nrf2	ACACGGTCCACAGCTCATC	TGTCAATCAAATCCATGTCCTG
NQO1	ATGTATGACAAAGGACCCTTCC	TCCCTTGCAGAGAGTACATGG
HO-1	AACTTTCAGAAGGGCCAGGT	CTGGGCTCTCCTTGTTGC
GST	GACTGCTTTCTTCAGGGTTCAAG	TCTGTGTAATTCATGGCTGATTCC
GADPH	CTGACTTCAACAGCGACACC	TGCTGTAGCCAAATTCGTTGT

Nrf2, nuclear factor erythroid-2 related factor 2; NQO1, NAD(P)H dehydrogenase [quinone] 1; HO-1, heme oxygenase-1; GST, glutathione S-transferase; PCR, polymerase chain reaction.

Hercules, CA, USA) with GAPDH as an internal reference. The gray value of each target band was analyzed using ImageJ 1.43 software (National Institutes of Health, Bethesda, MD, USA).

Flow cytometry. The 786-0 cells were separated into four groups: The control group (an untreated control), the sunitinib group [786-0 cells treated with sunitinib (IC_{50} 5.172 μmol/l)], the NC + sunitinib group (786-0 cells transfected with empty plasmid and treated with sunitinib) and the shRNA-Nrf2 + sunitinib group (786-0 cells transfected with shRNA-Nrf2 and treated with sunitinib). The 786-0 cells in each group in the logarithmic phase were collected and fixed with absolute alcohol at 4˚C overnight. The cells were washed with PBS and centrifuged for 5 min at 500 x g at 37˚C, following which the supernatant was removed. Cells were resuspended in 100 μl PBS followed by staining with propidium iodide (PI; 300 μl) in the Annexin V kit at 4˚C and 15 min incubation at room temperature in the dark. A flow cytometer (BD Pharmingen; BD Biosciences, San Jose, CA, USA) was used to determine cell cycle stage and the percentage of cells in each phase. An Annexin V kit (cat. no. C1063; Beyotime Institute of Biotechnology, Beijing, China) was used to detect apoptotic cells. The apoptotic rate was calculated as follows: Early apoptosis rate [Annexin V-fluorescein isothiocyanate (FITC) positive/PI negative] + late apoptosis rate (Annexin V-FITC positive/PI positive). Cell culture medium in 6-well plates was removed into centrifuge tubes and digested with 0.25% trypsin. Following trypsinization, the supernatant was extracted to add into the originally collected culture medium, and a 5 min centrifugation at 3,600 g at 4˚C was performed to collect the cell precipitate. PBS was added to resuspend the cell precipitate as a 50-100,000 cell solution. The resuspended cells were added to a final volume of 300 μl with Annexin V-FITC and PI, incubated at 4˚C in the dark for 30 min, and detected using a flow cytometer (BD Pharmingen; BD Biosciences) with a post-ice bath. Cell Quest 3.0 software (Becton-Dickinson and Company, Franklin Lakes, NJ, USA) was used to analyze the results.

Gene perturbation analysis. Gene Perturbation Atlas 1.0 (GPA; http://biocc.hrbmu.edu.cn/GPA/) software was used to evaluate the perturbation of gene interaction subnetworks. For each perturbed gene, its directly interacting genes and DEGs, at a distance of two steps, in the protein interaction network were extracted to construct its initiated subnetwork.

Statistical analysis. Statistical analysis was performed using SPSS 19.0 software (IBM Corp., Armonk, NY, USA). Each experiment was repeated in triplicate. The measurement data in a normal distribution is presented as the mean ± standard deviation. Differences between two groups were compared using the t-test. One-way analysis of variance (ANOVA) with Tukey's honestly significant difference (HSD) post hoc test was used to analyze multiple comparisons. The enumeration data are expressed as a percentage and ration, and were analyzed using the χ^2 test. Survival rate curves were plotted according to the Kaplan-Meier method and compared by the log-rank test. The IC_{50} of 786-0 cells was calculated using GraphPad Prism 6.0 software (GraphPad Software, Inc., La Jolla, CA, USA). $P<0.05$ was considered to indicate a statistically significant difference.

Results

Nrf2, NQO1 and HO-1 protein expression in RCC. Nrf2 is a critical transcription regulator of a series of antioxidants and detoxification enzymes that serve critical roles in regulating the sensitivity of chemotherapeutic agents (13,25). By uncoupling with Kelch-like ECH-associated protein 1 (Keap1), Nrf2 initiates the expression of antioxidant genes, including NQO1 and HO-1 (26,27). The protein expression of Nrf2, NQO1 and HO-1 was examined in RCC tissues and adjacent tissues. The results demonstrated that Nrf2, NQO1 and HO-1 were weakly stained in adjacent tissues, whereas in RCC tissues they were markedly stained sepia in the cytoplasm (Fig. 1A). The statistical analysis demonstrated that the positive rates of Nrf2, NQO1 and HO-1 in adjacent tissues and RCC tissues was 30.56 vs. 75.93, 22.22 vs. 69.44 and 36.11 vs. 72.22, respectively (data not shown). When the number of patients with positive staining in RCC tissues was compared with the adjacent tissues, the expression of Nrf2, NQO1 and HO-1 was significantly increased in RCC tissues (χ^2 test; all $P<0.05$). As presented in Fig. 1B, the Kaplan-Meier survival rate curve indicated that the patients with negative Nrf2, NQO1 or HO-1 expression had longer OS compared with patients with positive expression of Nrf2, NQO1 or HO-1, respectively, (log-rank test; all $P<0.05$) according to the 5-year follow-ups of patients with RCC.

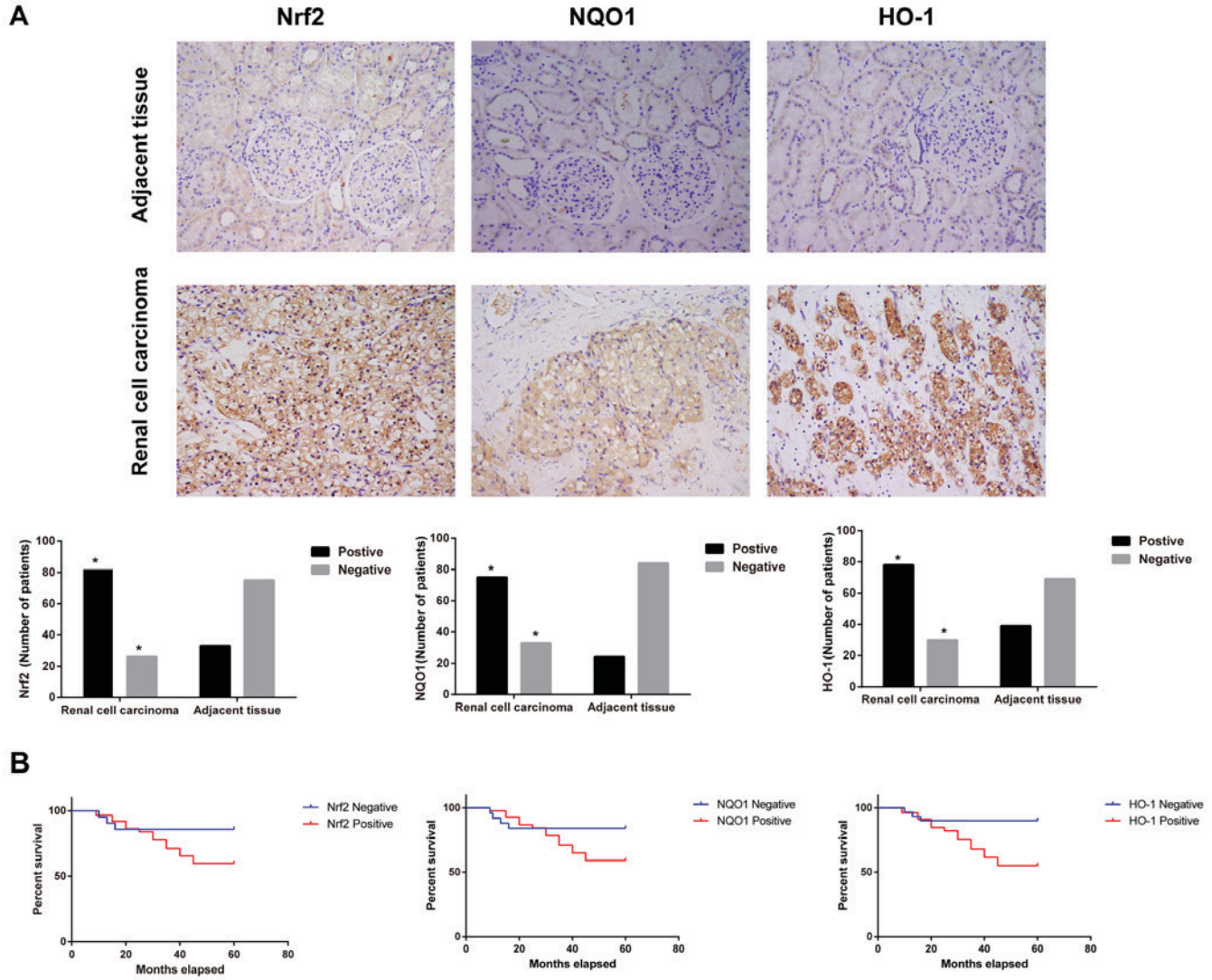

Figure 1. Expression of Nrf2, NQO1 and HO-1 in RCC tissues and adjacent tissues. (A) Expression of Nrf2, NQO1 and HO-1 in RCC tissues and adjacent tissues as detected by immunohistochemistry. Magnification, x200. *P<0.05, compared with the adjacent tissues. (B) Effects of Nrf2, NQO1 and HO-1 expression on the survival of patients with RCC. Nrf2, nuclear factor erythroid-2 related factor 2; NQO1, NAD(P)H dehydrogenase [quinone] 1; HO-1, heme oxygenase-1; RCC, renal cell carcinoma.

Associations of Nrf2-ARE signaling pathway-associated protein expression and clinicopathological features in RCC. Table II demonstrates that the expression levels of Nrf2, NQO1 and HO-1 were not significantly different according to age, sex or pathological type (χ^2 test; all P>0.05); however, were significantly different according to TNM stage, Fuhrman classification and lymph node metastasis (χ^2 test; all P<0.05). Additionally, the positive rates of Nrf2, NQO1 and HO-1 in patients at stage III-IV (TNM staging), at grade III+IV (Fuhrman classification) and with lymph node metastasis were significantly higher compared with patients at stage I-II, at grade I+II and without lymph node metastasis, respectively (χ^2 test; all P<0.05).

Expression levels of Nrf2, NQO1 and HO-1 in different RCC cell lines. As presented in Fig. 2, when compared with the human kidney tubule epithelial cell line HK-2, Nrf2, NQO1 and HO-1 were all significantly upregulated at the mRNA and protein expression levels in ACHN, Caki-1, 769-P and 786-0 cells (one-way ANOVA; all P<0.05). The 786-0 cells exhibited the highest Nrf2, NQO1 and HO-1 mRNA and protein expression levels, thus the 786-0 cells were selected for further study.

Expression of mRNAs and proteins associated with the Nrf2-ARE signaling pathway following transfection with shRNA-Nrf2. Following transfection with shRNA-Nrf2, western blotting and RT-qPCR were performed to detect the Nrf2-ARE signaling-associated proteins Nrf2, NQO1, HO-1 and GST at the mRNA and protein expression levels. Compared with the mock group, Nrf2, NQO1, HO-1 and GST were significantly decreased at the mRNA and protein expression levels in the shRNA-Nrf2 group (Tukey's HSD post hoc test; all P<0.05). As presented in Fig. 3, Nrf2 was significantly downregulated in the shRNA-Nrf2 group compared with the mock group (Tukey's HSD post hoc test; P<0.05); however, no observable difference was identified between the mock group and the NC group (Tukey's HSD post hoc test; P>0.05). The mRNA and protein expression levels of Nrf2, NQO1, HO-1 and GST were not significantly different between

Table II. Correlations of expression levels of Nrf2, NQO1 and HO-1, and clinicopathological features in renal cell carcinoma.

		Nrf2		NQO1		HO-1	
Variables	n	Positive cases (%)	P-value	Positive cases (%)	P-value	Positive cases (%)	P-value
Sex			0.539		0.339		0.749
Male	78	58 (74.36)		51 (87.93)		57 (73.08)	
Female	30	24 (80.00)		24 (80.00)		21 (70.00)	
Age			0.664		0.907		0.962
<50	50	37 (74.00)		35 (70.00)		36 (72.00)	
≥50	58	45 (77.59)		40 (68.97)		42 (72.41)	
Pathological types			0.795		0.399		0.804
Clear cell carcinoma	81	61 (75.31)		58 (71.60)		59 (72.84)	
Non-clear cell carcinoma	27	21 (77.78)		17 (62.96)		19 (70.37)	
Fuhrman classification			0.018		0.003		0.039[a]
I+II	66	45 (68.18)		39 (59.09)		43 (65.15)	
III+IV	42	37 (88.10)		36 (85.71)[a]		35 (83.33)[a]	
TNM staging			0.010		0.021		0.022[a]
I-II	64	43 (67.19)		39 (60.94)		41 (64.06)	
III-IV	44	39 (88.64)		36 (81.82)[a]		37 (84.09)[a]	
Lymph node metastasis			<0.001		<0.001		<0.001[a]
Positive	29	29 (100.00)		29 (100.00)		28 (96.55)	
Negative	79	53 (67.09)		46 (58.23)[a]		50 (63.29)[a]	

Nrf2, nuclear factor erythroid-2 related factor 2; NQO1, NAD(P)H dehydrogenase [quinone] 1; HO-1, heme oxygenase-1; TNM, tumor node metastasis; [a]P<0.05.

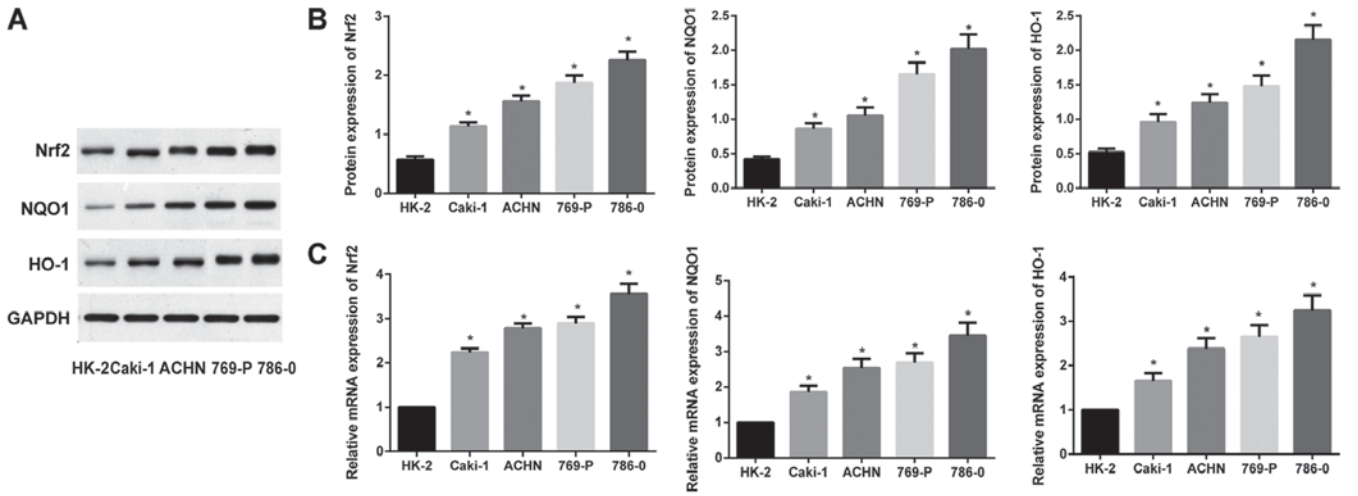

Figure 2. Expression of Nrf2, NQO1 and HO-1 in the human kidney tubule epithelial cell line HK-2 and RCC cell lines Caki-1, ACHN, 769-P and 786-0. (A) Nrf2, NQO1 and HO-1 protein expression in different cell lines as detected by western blotting. Comparison of the (B) protein and (C) mRNA expression levels of Nrf2, NQO1 and HO-1 among different cell lines. *P<0.05 vs. HK-2 cells. Nrf2, nuclear factor erythroid-2 related factor 2; NQO1, NAD(P)H dehydrogenase [quinone] 1; HO-1, heme oxygenase-1; RCC, renal cell carcinoma.

the mock group and the NC group (Tukey's HSD post hoc test; all P>0.05; Fig. 3).

Effects of shRNA-Nrf2 transfection on the viability of 786-0 cells. The CCK-8 assay demonstrated no significant differences in cell viabilities (24, 48 and 72 h) between the mock group and the NC group (Tukey's HSD post hoc test; all P>0.05). However, the cell viabilities of 786-0 cells at 24, 48 and 72 h were significantly decreased in the shRNA-Nrf2 group compared with the mock group (Tukey's HSD post hoc test; all P<0.05 Fig. 4).

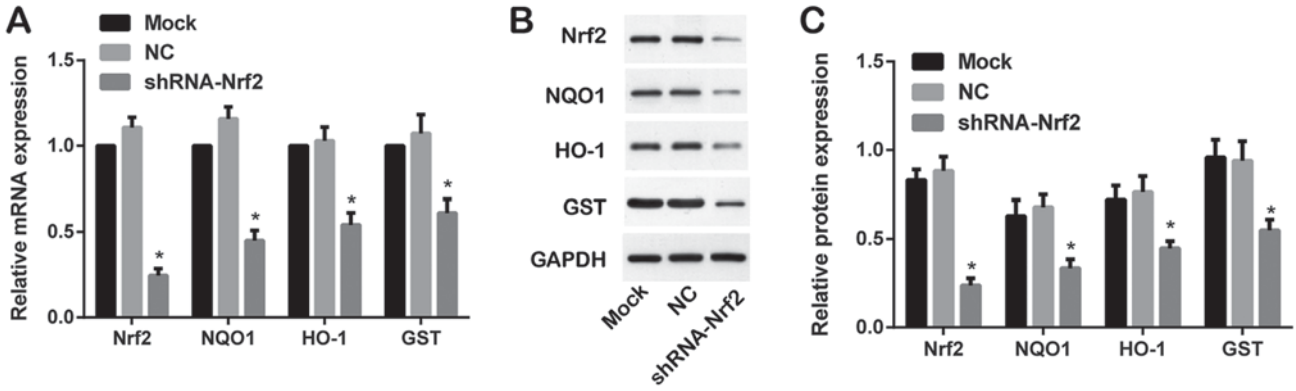

Figure 3. Expression of Nrf2-ARE-associated proteins and mRNAs in each group as detected by western blotting and RT-qPCR. (A) Expression of Nrf2, NQO1, HO-1 and GST mRNAs in each group as detected by RT-qPCR. (B) Expression of Nrf2, NQO1, HO-1 and GST proteins in each group as detected by western blotting. (C) Relative expression of Nrf2, NQO1, HO-1 and GST proteins in each group as detected by western blotting and subsequent densitometry analysis. *P<0.05 vs. respective mock group. Nrf2, nuclear factor erythroid-2 related factor 2; ARE, antioxidant-responsive element; NQO1, NAD(P)H dehydrogenase [quinone] 1; HO-1, heme oxygenase-1; GST, glutathione S-transferase; RT-qPCR, reverse transcription-quantitative polymerase chain reaction.

Transcriptome analysis results of Nrf2 knockdown. GPA software was used to evaluate the perturbation of gene interaction subnetworks (Fig. 5). In the perturbation of Nrf2 in the human lung cancer cell line A549 (GPA ID: GPAHSA000454), the downregulation of Nrf2 markedly decreased the expression of glutathione pathway genes, antioxidant enzymes and multidrug resistance proteins.

Effects of shRNA-Nrf2 transfection on the invasive and migratory abilities of 786-0 cells. The invasive ability of 786-0 cells, assessed by a Matrigel™ chamber invasion assay (Fig. 6A), demonstrated that a large number of cells migrated in the mock group and NC group, whereas, significantly less cell migration was observed in the shRNA-Nrf2 group (Tukey's HSD post hoc test; both P<0.05). The mock group and NC group demonstrated no significant difference (Tukey's HSD post hoc test; P>0.05). The scratch wound healing at 0 and 24 h, detected by a scratch assay (Fig. 6B), demonstrated that compared with the mock group and the NC group, the relative wound closure rate was significantly decreased in the shRNA-Nrf2 group (Tukey's HSD post hoc test; all P<0.05). The differences between the mock group and NC group were not statistically significant (Tukey's HSD post hoc test; P>0.05).

Comparison of sensitivities to targeted drug sunitinib following transfection with shRNA-Nrf2. Following transfection with shRNA-Nrf2, a CCK-8 assay was performed to detect the effects of the targeted drug sunitinib at different concentrations on the proliferation of 786-0 cells at different time points in each group. The CCK-8 assay results (Fig. 7) demonstrated that the cell viability significantly decreased in the shRNA-Nrf2 group compared with the NC group under the same concentration of sunitinib at 24 h (t-test; all P<0.05), and similar results were additionally observed at 48 and 72 h (t-test; all P<0.05), suggesting that sunitinib may inhibit cell growth in a dose dependent manner. The stronger inhibitory effect of sunitinib in the shRNA-Nrf2 group suggested that inhibition of Nrf2 expression increased the sensitivity to the targeted drug sunitinib. The IC_{50} of 786-0 cells at different time points was calculated in each group using GraphPad Prism 6.0 software. The IC_{50} values of sunitinib on 786-0 cells in the NC group were all significantly increased compared with those in the shRNA-Nrf2 group at 24, 48 and 72 h (t-test; all P<0.05). The above results demonstrated that 786-0 cells in the shRNA-Nrf2 group exhibited higher sensitivity to sunitinib.

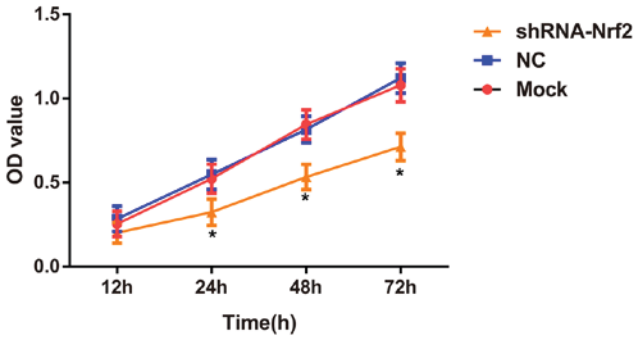

Figure 4. Effects of shRNA-Nrf2 transfection on proliferation of 786-0 cells in each group as detected by Cell Counting Kit-8. *P<0.05 vs. mock group. shRNA-Nrf2, small hairpin RNA-nuclear factor erythroid-2 related factor 2; NC, negative control; OD, optical density.

Effects of shRNA-Nrf2 transfection on the cell cycle and apoptosis of 786-0 cells. The IC_{50} of 786-0 cells at 48 h was 5.172 μmol/l, which was an effective concentration for altering the cell viability in the transfected cells in each group. Flow cytometry demonstrated that the ratio of cells in the G0/G1 phase was increased in the sunitinib group; however, the ratio of cells in the S and G2/M phases was decreased compared with the control group (Tukey's HSD post hoc test; all P<0.05). When compared with the sunitinib group, the ratio of cells in the G0/G1 phase was significantly increased, whereas, the ratio of cells in the S and G2/M phases was significantly decreased in the shRNA-Nrf2 + sunitinib group (Tukey's HSD post hoc test; all P<0.05). The differences between the sunitinib group and the NC + sunitinib group were not statistically significant (Tukey's HSD post hoc test; P>0.05; Fig. 8A). Higher rates of cell apoptosis were observed in the sunitinib group compared with the control group (Tukey's HSD post hoc test; P<0.05).

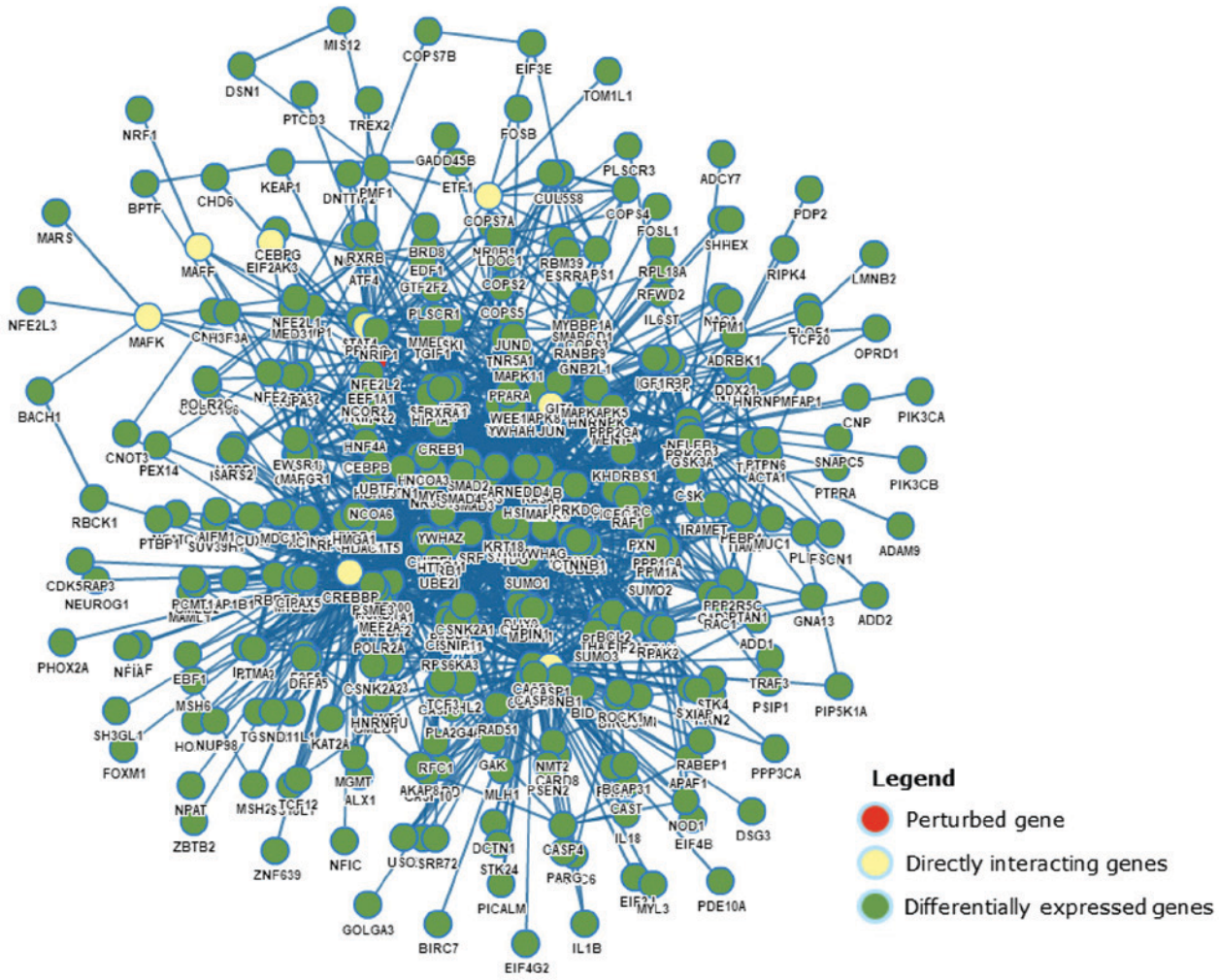

Figure 5. Transcriptome analysis results of nuclear factor erythroid-2 related factor 2 knockdown.

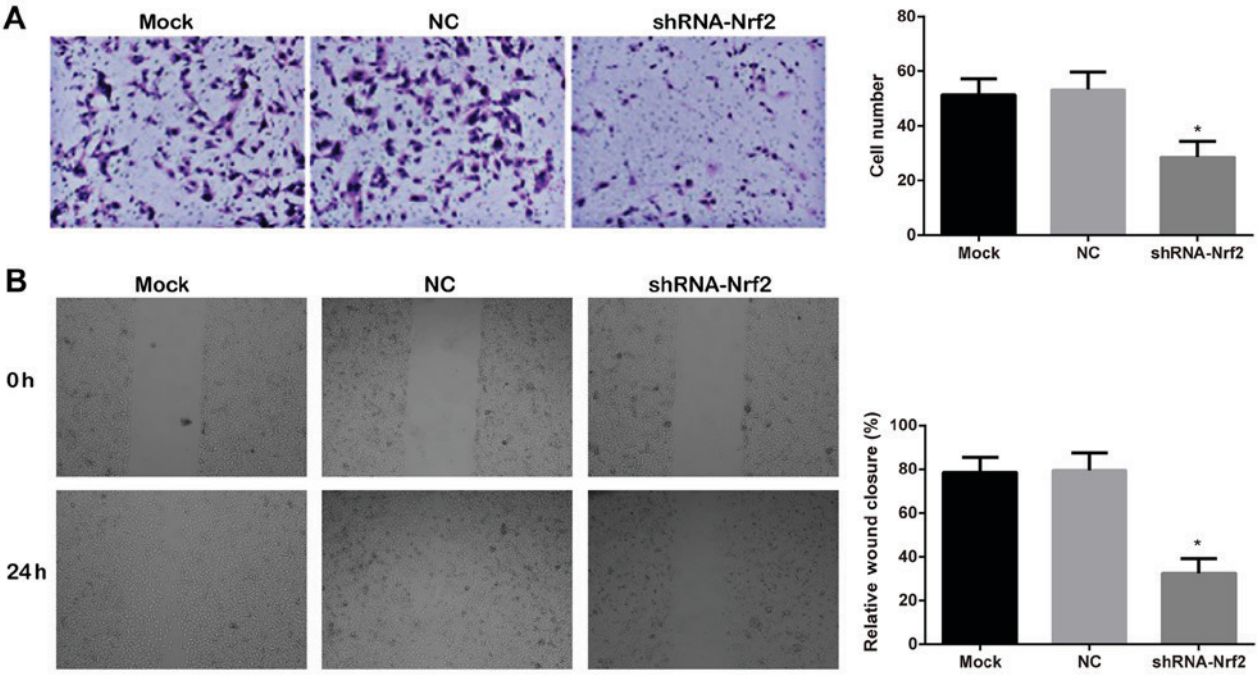

Figure 6. Effects of shRNA-Nrf2 transfection on the invasive and migratory abilities of 786-0 cells by a Matrigel™ and scratch assay. (A) Matrigel™ detection of invasive ability of 786-0 cells in each group. (B) Scratch assay to assess the migratory ability of 786-0 cells in each group. Magnification, x400. *P<0.05 vs. mock group. NC, negative control; shRNA-Nrf-2, small hairpin RNA-nuclear factor erythroid-2 related factor 2.

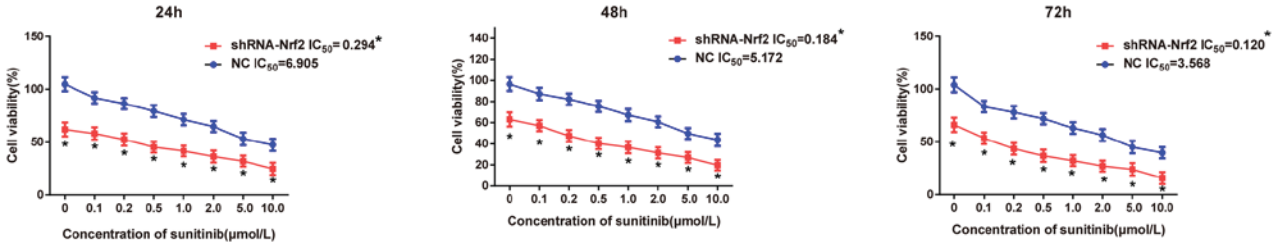

Figure 7. Comparison of sensitivity to different concentrations of sunitinib following shRNA-Nrf2 transfection in 786-0 cells as detected by Cell Counting Kit-8. *P<0.05 vs. respective NC. shRNA-Nrf2, small hairpin RNA-nuclear factor erythroid-2 related factor 2; NC, negative control; IC_{50}, half-maximal inhibitory concentration.

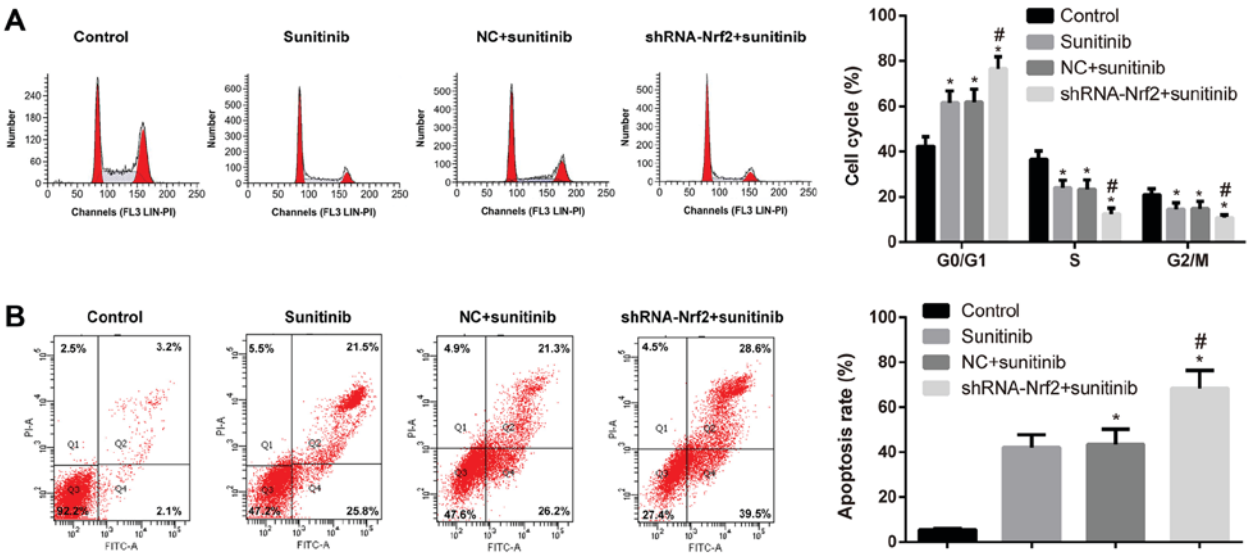

Figure 8. Comparison of cell cycle and apoptosis of 786-0 cells when treated with sunitinib (5.172 μmol/l) in different transfection groups. (A) In total, 10,000 cells were collected and analyzed by flow cytometry, and the cell cycle profiles were analyzed. (B) Detection of cell apoptosis in each group by flow cytometry. *P<0.05 vs. respective control group; #P<0.05 vs. respective sunitinib group. FITC, fluorescein isothiocyanate; PI, propidium iodide; NC, negative control; shRNA-Nrf2, small hairpin RNA-nuclear factor erythroid-2 related factor 2.

Similarly, compared with the sunitinib group, the cell apoptosis rate was significantly increased in the shRNA-Nrf2 + sunitinib group (Tukey's HSD post hoc test; all P<0.05). No significant difference in cell apoptosis was observed between the sunitinib group and the NC + sunitinib group (Tukey's HSD post hoc test; P>0.05; Fig. 8B).

Discussion

Nrf2 regulates and encodes antioxidant proteins through interactions with the ARE, one of the most important endogenous antioxidant stress pathways identified (28,29). The ARE regulates downstream antioxidant enzymes, including NQO1, HO-1, superoxide dismutase (SOD), various GST isozymes, and catalase (30). In the present study, the protein expression levels of Nrf2, NQO1 and HO-1 in RCC tissues were not only markedly higher compared with adjacent non-cancerous tissues, they were additionally associated with TNM stage, Fuhrman classification and lymph node metastasis in RCC, which is in agreement with the expression of Nrf2 signaling pathway components in other carcinomas, suggesting that Nrf2 is highly expressed in tumors (31,32). Multiple previous studies have demonstrated the carcinogenic effects of Nrf2. For example, Yoo *et al* (33) identified Nrf2 accumulation in gastric carcinoma tissues compared with normal gastric tissues. Additionally, in colonic carcinoma tissues, Nrf2 and NQO1 were upregulated (33,34). Specifically, the higher the Nrf2 expression was, the higher the Duke stage or the worse the prognosis was (34,35). Similarly, Nrf2 was positively expressed in human lung carcinoma, which was associated with worse prognosis (36). Therefore, Nrf2 and downstream target genes may possess vital roles in the occurrence, development and metastasis of RCC.

In the present study, it was identified that inhibition of Nrf2 expression not only suppressed the viability, invasion and migration of 786-0 cells; however, additionally downregulated NQO1, HO-1 and GST at the mRNA and protein expression levels. Kim *et al* (37) observed that the loss of E-cadherin may activate Nrf2, consequently promoting tumor growth and metastasis. In hepatocellular carcinoma, Nrf2 is able to upregulate the oncogene apoptosis regulator Bcl-2, and interference with Nrf2 expression leads to the apoptosis of cancer cells (38). In addition, the Nrf2-mediated antioxidant effect is primarily achieved by increasing glutathione biosynthesis and inducing phase II detoxifying enzymes, including GST, NAD(P)H dehydrogenase, NQO1, SOD, HO-1 and γ-glutamylcysteine

ligase (39,40). As one of the most important antioxidants in cells, glutathione functions via the reductive thiol on its cysteine, which may be reduced following oxidation (41). When cells are exposed to carcinogenic substances or oxidative stress stimulation, a carcinogen or an electrophile interacts with a cysteine of Keapl, the negative regulator of Nrf2, which causes the disruption of the Keap1 complex (42). This leads to decreased or even absent Keap1-dependent ubiquitination of Nrf2, release of Nrf2 from Keap1 inhibition, and the novel synthesized Nrf2 translocates to the nucleus (42). Nuclear accumulation of Nrf2 and binding to AREs in tumor cells results in increased glutathione levels, leading to upregulation of associated detoxifying enzymes and drug efflux pump genes, metabolic disorder of tumor cells and faster proliferation (43,44), further suggesting that Nrf2 serves as an oncogene to promote the migration and invasion of tumor cells, possibly via an increase in the tumor resistance to oxidative stress.

In the present study, it was additionally observed that inhibition of Nrf2 expression significantly increased the sensitivity of 786-0 cells to sunitinib at different concentrations, and shRNA-Nrf2 arrested 786-0 cells at G0/G1 phase to promote the apoptosis of RCC cells. Zhong *et al* (45) observed that silencing Nrf2 using siRNA enhanced the sensitivity of MCF-7 breast cancer cells to doxorubicin, paclitaxel and other chemotherapeutic agents. Kim *et al* (46) identified that in lung cancer cells, the Nrf2-HO-1 signal transduction pathway was closely correlated with the resistance of cancer cells to cisplatin, and inhibiting the expression or activity of HO-1 enhanced the sensitivity of A549 cells to cisplatin. Arlt *et al* (47) demonstrated that inhibition of Nrf2 activity in pancreatic cancer enhanced the sensitivity of anticancer drugs by suppressing tumor cell apoptosis. Therefore, inhibiting Nrf2 may be a novel and effective strategy to improve the sensitivity of cells to anticancer drugs (48). However, Nrf2 regulates certain genes involved in the phosphatidyl-inositol 3-kinase (PI3K)-protein kinase B (AKT) pathway (49,50), and the PI3K-AKT pathway is able to regulate biological processes, including cell proliferation, differentiation and apoptosis, in addition to being involved in oncogenesis, cancer progression and drug resistance in different cancer types (51-53). Notably, the PI3K-AKT pathway serves a crucial role in sunitinib resistance and is considered a potential drug target in renal cancer and other cancer types (54,55), suggesting that Nrf2 may contribute to sunitinib resistance by activating the PI3K-AKT pathway.

Sunitinib, a small-molecular multi-target anticancer drug, is able to block vascular endothelial growth factor, platelet-derived growth factor receptor α and β, reticulocyte, c-kit and other receptors, allowing it to serve as an anti-tumorigenic and anti-angiogenic reagent (56,57). Yang *et al* (58) observed that sunitinib enhanced the apoptosis of medulloblastoma by inhibiting the signal transducer and activator of transcription and PI3K-AKT signaling pathways. Furthermore, particulate matter with an aerodynamic diameter of <2.5 μm induced reactive oxygen species (ROS) generation, triggered the translocation of Nrf2 to the nucleus and increased HO-1 expression by mediating PI3K/AKT phosphorylation in A549 cells (59). At present, the primary mechanism of a number of anticancer drugs to induce cell apoptosis is the generation of ROS, suggesting that the Nrf2-ARE signaling pathway may regulate ROS production in tumor cells or the PI3K-AKT signaling pathway to affect the sensitivity of RCC cells to sunitinib (60), a possibility which warrants further experimentation. One of the limitations of the present study was the small sample, therefore further experiments are required with a larger sample size.

In conclusion, the Nrf2-ARE signaling pathway was activated in RCC, and inhibition of Nrf2-ARE signaling enhanced tumor resistance to oxidative stress, which not only suppressed the proliferation and metastasis of RCC cells; however, additionally increased the sensitivity of RCC cells to the targeted drug sunitinib. The present findings provide a theoretical basis from which novel mechanisms of resistance to targeted drug and novel molecular targets may be identified to enhance drug sensitivity in patients with RCC.

Acknowledgements

Not applicable.

Funding

The present study was supported by funding from Natural Science Foundation of Guangdong Province, China (grant no. 2015A030310460) and National Science Foundation of China (grant no. 81371387).

Availability of data and materials

The datasets used and/or analyzed during the current study are available from the corresponding author on reasonable request.

Authors' contributions

LY and YL were involved in the design of the study and performed the majority of the analyses. SJ drafted the manuscript. SJ, XZ and YX conceived and coordinated the study. All authors read and approved the final manuscript.

Ethics approval and consent to participate

The present study protocol was approved by the Ethics Committee of The First Affiliated Hospital of Soochow University, Suzhou, China (approval no. 2013031), and all research subjects provided written informed consent. All procedures in the present study strictly complied with the guidelines and principles of the Declaration of Helsinki.

Patient consent for publication

The present study was granted an exemption by the Ethics Committee of The First Affiliated Hospital of Soochow University, as the patients cannot be traced.

Competing interests

The authors declare that they have no competing interests.

References

1. Lipworth L, Tarone RE and McLaughlin JK: The epidemiology of renal cell carcinoma. J Urol 176: 2353-2358, 2006.

2. Zheng B, Zhu H, Gu D, Pan X, Qian L, Xue B, Yang D, Zhou J and Shan Y: MiRNA-30a-mediated autophagy inhibition sensitizes renal cell carcinoma cells to sorafenib. Biochem Biophys Res Commun 459: 234-239, 2015.
3. Gupta K, Miller JD, Li JZ, Russell MW and Charbonneau C: Epidemiologic and socioeconomic burden of metastatic renal cell carcinoma (mRCC): A literature review. Cancer Treat Rev 34: 193-205, 2008.
4. Breau RH and Blute ML: Surgery for renal cell carcinoma metastases. Curr Opin Urol 20: 375-381, 2010.
5. Bukowski RM: Systemic therapy for metastatic renal cell carcinoma in treatment naive patients: A risk-based approach. Expert Opin Pharmacother 11: 2351-2362, 2010.
6. Motzer RJ, Jonasch E, Agarwal N, Beard C, Bhayani S, Bolger GB, Chang SS, Choueiri TK, Costello BA, Derweesh IH, *et al*: Kidney cancer, version 3.2015. J Natl Compr Canc Netw 13: 151-159, 2015.
7. Achermann C, Stenner F and Rothschild SI: Treatment, outcome and prognostic factors in renal cell carcinoma-A single center study (2000-2010). J Cancer 7: 921-927, 2016.
8. Sonpavde G, Choueiri TK, Escudier B, Ficarra V, Hutson TE, Mulders PF, Patard JJ, Rini BI, Staehler M, Sternberg CN and Stief CG: Sequencing of agents for metastatic renal cell carcinoma: Can we customize therapy? Eur Urol 61: 307-316, 2012.
9. M Eel D: Utilization of sunitinib for renal cell cancer: An egyptian university hospital experience. Asian Pac J Cancer Prev 17: 3161-3166, 2016.
10. Zheng WX, Yan F, Xue Q, Wu GJ, Qin WJ, Wang FL, Qin J, Tian CJ and Yuan JL: Heme oxygenase-1 is a predictive biomarker for therapeutic targeting of advanced clear cell renal cell carcinoma treated with sorafenib or sunitinib. Onco Targets Ther 8: 2081-2088, 2015.
11. Rini BI and Atkins MB: Resistance to targeted therapy in renal-cell carcinoma. Lancet Oncol 10: 992-1000, 2009.
12. Buczek M, Escudier B, Bartnik E, Szczylik C and Czarnecka A: Resistance to tyrosine kinase inhibitors in clear cell renal cell carcinoma: From the patient's bed to molecular mechanisms. Biochim Biophys Acta 1845: 31-41, 2014.
13. Jaramillo MC and Zhang DD: The emerging role of the Nrf2-Keap1 signaling pathway in cancer. Genes Dev 27: 2179-2191, 2013.
14. Magesh S, Chen Y and Hu L: Small molecule modulators of Keap1-Nrf2-ARE pathway as potential preventive and therapeutic agents. Med Res Rev 32: 687-726, 2012.
15. Calkins MJ, Johnson DA, Townsend JA, Vargas MR, Dowell JA, Williamson TP, Kraft AD, Lee JM, Li J and Johnson J: The Nrf2/ARE pathway as a potential therapeutic target in neurodegenerative disease. Antioxid Redox Signal 11: 497-508, 2009.
16. Ji L, Li H, Gao P, Shang G, Zhang DD, Zhang N and Jiang T: Nrf2 pathway regulates multidrug-resistance-associated protein 1 in small cell lung cancer. PLoS One 8: e63404, 2013.
17. Kim TH, Hur EG, Kang SJ, Kim JA, Thapa D, Lee YM, Ku SK, Jung Y and Kwak M: NRF2 blockade suppresses colon tumor angiogenesis by inhibiting hypoxia-induced activation of HIF-1α. Cancer Res 71: 2260-2275, 2011.
18. Samatiwat P, Prawan A, Senggunprai L and Kukongviriyapan V: Repression of Nrf2 enhances antitumor effect of 5-fluorouracil and gemcitabine on cholangiocarcinoma cells. Naunyn Schmiedebergs Arch Pharmacol 388: 601-612, 2015.
19. Akhdar H, Loyer P, Rauch C, Corlu A, Guillouzo A and Morel F: Involvement of Nrf2 activation in resistance to 5-fluorouracil in human colon cancer HT-29 cells. Eur J Cancer 45: 2219-2227, 2009.
20. Muglia VF and Prando A: Renal cell carcinoma: Histological classification and correlation with imaging findings. Radiol Bras 48: 166-174, 2015.
21. Moch H, Artibani W, Delahunt B, Ficarra V, Knuechel R, Montorsi F, Patard JJ, Stief CG, Sulser T and Wild PJ: Reassessing the current UICC/AJCC TNM staging for renal cell carcinoma. Eur Urol 56: 636-643, 2009.
22. Tan EY, Campo L, Han C, Turley H, Pezzella F, Gatter KC, Harris AL and Fox SB: BNIP3 as a progression marker in primary human breast cancer; opposing functions in in situ versus invasive cancer. Clin Cancer Res 13: 467-474, 2007.
23. Ooi A, Dykema K, Ansari A, Petillo D, Snider J, Kahnoski R, Anema J, Craig D, Carpten J, Teh BT and Furge KA: CUL3 and NRF2 mutations confer an NRF2 activation phenotype in a sporadic form of papillary renal cell carcinoma. Cancer Res 73: 2044-2051, 2013.
24. Livak KJ and Schmittgen TD: Analysis of relative gene expression data using real-time quantitative PCR and the 2(-Delta Delta C(T)) method. Methods 25: 402-408, 2001.
25. Gu S, Lai Y, Chen H, Liu Y and Zhang Z: miR-155 mediates arsenic trioxide resistance by activating Nrf2 and suppressing apoptosis in lung cancer cells. Sci Rep 7: 12155, 2017.
26. Lu MC, Ji JA, Jiang ZY and You QD: The Keap1-Nrf2-ARE pathway as a potential preventive and therapeutic target: An update. Med Res Rev 36: 924-963, 2016.
27. Liu D, Duan X, Dong D, Bai C, Li X, Sun G and Li B: Activation of the Nrf2 pathway by inorganic arsenic in human hepatocytes and the role of transcriptional repressor Bach1. Oxid Med Cell Longev 2013: 984546, 2013.
28. Deng C, Tao R, Yu SZ and Jin H: Inhibition of 6-hydroxydopamine-induced endoplasmic reticulum stress by sulforaphane through the activation of Nrf2 nuclear translocation. Mol Med Rep 6: 215-219, 2012.
29. Ildefonso CJ, Jaime H, Brown EE, Iwata RL, Ahmed CM, Massengill MT, Biswal MR, Boye SE, Hauswirth WW, Ash JD, *et al*: Targeting the Nrf2 signaling pathway in the retina with a gene-delivered secretable and cell-penetrating peptide. Invest Ophthalmol Vis Sci 57: 372-386, 2016.
30. Wan Hasan WN, Kwak MK, Makpol S, Wan Ngah WZ and Mohd Yusof YA: Piper betle induces phase I & II genes through Nrf2/ARE signaling pathway in mouse embryonic fibroblasts derived from wild type and Nrf2 knockout cells. BMC Complement Altern Med 14: 72, 2014.
31. Hayes JD and McMahon M: NRF2 and KEAP1 mutations: Permanent activation of an adaptive response in cancer. Trends Biochem Sci 34: 176-188, 2009.
32. Geismann C, Arlt A, Sebens S and Schäfer H: Cytoprotection 'gone astray': Nrf2 and its role in cancer. Onco Targets Ther 7: 1497-1518, 2014.
33. Yoo NJ, Kim YR and Lee SH: Expression of NRF2, a cytoprotective protein, in gastric carcinomas. APMIS 118: 613-614, 2010.
34. Ji L, Wei Y, Jiang T and Wang S: Correlation of Nrf2, NQO1, MRP1, cmyc and p53 in colorectal cancer and their relationships to clinicopathologic features and survival. Int J Clin Exp Pathol 7: 1124-1131, 2014.
35. Wang J, Zhang M, Zhang L, Cai H, Zhou S, Zhang J and Wang Y: Correlation of Nrf2, HO-1, and MRP3 in gallbladder cancer and their relationships to clinicopathologic features and survival. J Surg Res 164: e99-e105, 2010.
36. Solis LM, Behrens C, Dong W, Suraokar M, Ozburn NC, Moran CA, Corvalan AH, Biswal S, Swisher SG, Bekele BN, *et al*: Nrf2 and Keap1 abnormalities in non-small cell lung carcinoma and association with clinicopathologic features. Clin Cancer Res 16: 3743-3753, 2010.
37. Kim WD, Kim YW, Cho IJ, Lee CH and Kim SG: E-cadherin inhibits nuclear accumulation of Nrf2: Implications for chemoresistance of cancer cells. J Cell Sci 125: 1284-1295, 2012.
38. Niture SK and Jaiswal AK: Nrf2 protein up-regulates antiapoptotic protein Bcl-2 and prevents cellular apoptosis. J Biol Chem 287: 9873-9886, 2012.
39. Rotblat B, Melino G and Knight RA: NRF2 and p53: Januses in cancer? Oncotarget 3: 1272-1283, 2012.
40. Zhang M, An C, Gao Y, Leak RK, Chen J and Zhang F: Emerging roles of Nrf2 and phase II antioxidant enzymes in neuroprotection. Prog Neurobiol 100: 30-47, 2013.
41. Aborode FA, Raab A, Voigt M, Costa LM, Krupp EM and Feldmann J: The importance of glutathione and phytochelatins on the selenite and arsenate detoxification in Arabidopsis thaliana. J Environ Sci (China) 49: 150-161, 2016.
42. Niture SK, Kaspar JW, Shen J and Jaiswal AK: Nrf2 signaling and cell survival. Toxicol Appl Pharmacol 244: 37-42, 2010.
43. DeNicola GM, Karreth FA, Humpton TJ, Gopinathan A, Wei C, Frese K, Mangal D, Yu KH, Yeo CJ, Calhoun ES, *et al*: Oncogene-induced Nrf2 transcription promotes ROS detoxification and tumorigenesis. Nature 475: 106-109, 2011.
44. Mitsuishi Y, Taguchi K, Kawatani Y, Gopinathan A, Wei C, Frese K, Mangal D, Yu KH, Yeo CJ and Calhoun ES: Nrf2 redirects glucose and glutamine into anabolic pathways in metabolic reprogramming. Cancer Cell 22: 66-79, 2012.
45. Zhong Y, Zhang F, Sun Z, Zhou W, Li ZY, You QD, Guo QL and Hu R: Drug resistance associates with activation of Nrf2 in MCF-7/DOX cells, and wogonin reverses it by down-regulating Nrf2-mediated cellular defense response. Mol Carcinog 52: 824-834, 2013.

46. Kim HR, Kim S, Kim EJ, Park JH, Yang SH, Jeong ET, Park C, Youn MJ, So HS and Park R: Suppression of Nrf2-driven heme oxygenase-1 enhances the chemosensitivity of lung cancer A549 cells toward cisplatin. Lung Cancer 60: 47-56, 2008.
47. Arlt A, Sebens S, Krebs S, Geismann C, Grossmann M, Kruse ML, Schreiber S and Schäfer H: Inhibition of the Nrf2 transcription factor by the alkaloid trigonelline renders pancreatic cancer cells more susceptible to apoptosis through decreased proteasomal gene expression and proteasome activity. Oncogene 32: 4825-4835, 2013.
48. Li QK, Singh A, Biswal S, Askin F and Gabrielson E: KEAP1 gene mutations and NRF2 activation are common in pulmonary papillary adenocarcinoma. J Hum Genet 56: 230-234, 2011.
49. Lim JH, Kim KM, Kim SW, Hwang O and Choi HJ: Bromocriptine activates NQO1 via Nrf2-PI3K/Akt signaling: Novel cytoprotective mechanism against oxidative damage. Pharmacol Res 57: 325-331, 2008.
50. Zhang Y, Guan L, Wang X, Wen T, Xing J and Zhao J: Protection of chlorophyllin against oxidative damage by inducing HO-1 and NQO1 expression mediated by PI3K/Akt and Nrf2. Free Radic Res 42: 362-371, 2008.
51. Mayer IA and Arteaga CL: The PI3K/AKT pathway as a target for cancer treatment. Annu Rev Med 67: 11-28, 2016.
52. Chang F, Lee JT, Navolanic PM, Steelman LS, Shelton JG, Blalock WL, Franklin RA and McCubrey JA: Involvement of PI3K/Akt pathway in cell cycle progression, apoptosis, and neoplastic transformation: A target for cancer chemotherapy. Leukemia 17: 590-603, 2003.
53. West KA, Castillo SS and Dennis PA: Activation of the PI3K/Akt pathway and chemotherapeutic resistance. Drug Resist Updat 5: 234-248, 2002.
54. Makhov PB, Golovine K, Kutikov A, Teper E, Canter DJ, Simhan J, Uzzo RG and Kolenko VM: Modulation of Akt/mTOR signaling overcomes sunitinib resistance in renal and prostate cancer cells. Mol Cancer Ther 11: 1510-1517, 2012.
55. Chen YL, Ge GJ, Qi C, Wang H, Wang HL, Li LY, Li GH and Xia LQ: A five-gene signature may predict sunitinib sensitivity and serve as prognostic biomarkers for renal cell carcinoma. J Cell Physiol 233: 6649-6660, 2018.
56. Imbulgoda A, Heng DY and Kollmannsberger C: Sunitinib in the treatment of advanced solid tumors. Recent Results Cancer Res 201: 165-184, 2014.
57. Grassi P, Verzoni E, Porcu L, Iacovelli R, de Braud F and Procopio G: Sites of disease as predictors of outcome in metastatic renal cell carcinoma patients treated with first-line sunitinib or sorafenib. Ther Adv Urol 7: 59-68, 2015.
58. Yang F, Jove V, Xin H, Hedvat M, Van Meter TE and Yu H: Sunitinib induces apoptosis and growth arrest of medulloblastoma tumor cells by inhibiting STAT3 and AKT signaling pathways. Mol Cancer Res 8: 35-45, 2010.
59. Deng X, Rui W, Zhang F and Ding W: PM2.5 induces Nrf2-mediated defense mechanisms against oxidative stress by activating PIK3/AKT signaling pathway in human lung alveolar epithelial A549 cells. Cell Biol Toxicol 29: 143-157, 2013.
60. Singh A, Boldin-Adamsky S, Thimmulappa RK, Rath SK, Ashush H, Coulter J, Blackford A, Goodman SN, Bunz F, Watson WH, *et al*: RNAi-mediated silencing of nuclear factor erythroid-2-related factor 2 gene expression in non-small cell lung cancer inhibits tumor growth and increases efficacy of chemotherapy. Cancer Res 68: 7975-7984, 2008.